COBEM 2023 27TH INTERNATIONAL CONGRESS OF MECHANICAL ENGENEERING

ABCM Brazilian Society of Mechanical Sciences and Engineering
27th ABCM International Congress of Mechanical Engineering
December 04-08, 2023, Florianópolis-SC, Brazil

COB-2023-0141
A STUDY OF BOUNDARY LAYER DEVELOPING UNDER ADVERSE PRESSURE GRADIENTS FOR A NACA0012 AIRFOIL AT HIGH ANGLE OF ATTACK

Leandro Júnio de O. Silva
William R. Wolf
University of Campinas, Campinas, SP, 13083-860, Brazil
l184929@dac.unicamp.br, wolf@fem.unicamp.br

Abstract. *A wall-resolved large eddy simulation (LES) is applied to investigate the effects of varying adverse pressure gradients (APGs) on a turbulent boundary layer developing over an airfoil NACA0012 at* 9 *deg. angle of attack, Reynolds number of* $Re_c = 400,000$ *and freestream Mach number* $M_\infty = 0.2$*. The impact of the APG on the integral quantities of the boundary layer are investigated, as well as the Clauser pressure-gradient parameter. Turbulence statistics are evaluated in terms of the inner-scaled mean velocity profiles and Reynolds-stress tensors. These statistics are compared at different positions along the airfoil chord which allows an evaluation of the influence of different APGs. Due to the effects of the APGs, the mean velocity profiles present a downward shift in the log-layer and the normalized velocity in the potential flow region increases. The Reynolds-stress tensor components also increase due to pressure gradient effects and the tangential component presents a secondary peak in the outer layer.*

Keywords: *adverse pressure-gradient, boundary-layer, LES, turbulence*

1. INTRODUCTION

Turbulent boundary layers (TBLs) developing under different pressure gradients are present in several industrial applications including wings and rotor blades. These devices are used both in the aeronautical and energy industries and, therefore, their design is carried out with the aim of achieving the highest efficiency to reduce operational costs and emissions. Favorable pressure gradients (FPGs) may induce higher friction and drag while keeping the flow attached and if it is large enough it can cause relaminarization (Bourassa and Thomas, 2009). On the other hand, adverse pressure gradients (APGs) may cause flow separation and stall, inducing an increase in pressure drag.

Primary studies were performed by Clauser (1954, 1956) in which, through experimental investigations, he defined the pressure-gradient parameter β which gives the magnitude of the pressure gradient in TBLs. This parameter became known later as the Clauser parameter. Bradshaw (1967) made meansurements in three different boundary layers, one with zero pressure gradient (ZPG) and two with moderate and strong APG. In this study, he observed a low-frequency content rising in the TBLs outer regions as the pressure gradient was increased. Another important contribution on the study of TBLs subjected to APGs was provided by Nagano *et al.* (1993) where the authors showed experimentally that the turbulence statistics are greatly affected by increasing the APG. At the same time, Spalart and Watmuff (1993) used both experimental measurements and direct numerical simulations (DNS) to show the vertical downward shift of the inner-scaled mean velocity profile in the buffer and log layer regions as an effect of APGs. Futhermore, Skåre and Krogstad (1994) demonstrated experimentally that the APG influenced the production and dissipation term of turbulent kinect energy budget, increasing these terms in the near-wall region and in the outer layer.

The effects of APG in TBLs was also studied by Lee and Sung (2008) through direct numerical simualtions. Their results were comparted to ZPG calculations and it was shown that the APGs induce the formation of a secondary peak in the Reynolds stress distributions along the outer layer. They also showed that the standard logarithmic law-of-the-wall was not valid for APG flows. Moreover, Monty *et al.* (2011) presented experimentally that large-scales motions are energized by the pressure gradient, which leads to a mechanism that contributes to the increase in the turbulence intensity. Harun *et al.* (2013) also demonstrated experimentally that there is an increase in turbulence intensity on the outer-layer as the pressure gradient increases from favourable to adverse.

More recently, Vinuesa *et al.* (2017a) performed a DNS to evaluate the pressure gradient effects in a TBL developing over a NACA4412 airfoil. Their results showed the development of an outer peak in the Reynolds stress tensor distributions and an increased production and dissipation across the boundary layer attributed to the more intense large-scale motions of the APG flow. Subsequently, Vinuesa *et al.* (2017b) studied several experimental and numerical datasets with the aim of establishing a criterion of convergence to well-behavied conditions based on the Clauser pressure-gradient parameter β. Futhermore, the authors also used the skin-friction coefficient C_f and Re_θ to evaluate whether a TBL subjected to an APG could be considered well-behaved, i.e., the flow is independent of the inflow conditions and numerical or

experimental artifacts. Tanarro *et al.* (2020) performed a LES of NACA0012 and NACA4412 airfoil profiles and observed an interaction between the outer and near-wall regions. Their results demonstrated that the small scales near the wall are transported to the outer layer by the APG and, the energization mechanism of an APG is different from that observed for high Reynolds number flows.

In view of the above, the importance of studying TBLs subjected to APGs is clear. Therefore, the main goal of this work is to evaluate the effects of APGs on the boundary layer turbulence statistics. We investigate TBLs over an airfoil profile at a high angle of attack, but without mean flow separation. Hence, the present APGs develop in a situation where the deflection of streamlines is also important. A wall-resolved LES is performed for a NACA0012 profile at 9 deg. angle of attack. The Reynolds and Mach numbers are set as $Re_c = 400,000$ and $M_\infty = 0.2$, respectively, and tripping is enforced near the leading edge to guarantee the development of a fully turbulent boundary layer along the airfoil.

2. NUMERICAL METHODOLOGY

2.1 Large eddy simulation

The influence of the APG developing in a TBL on a NACA0012 airfoil at 9 deg. angle of attack is analyzed through the application of a wall-resolved Large Eddy Simulation (LES). The LES solves the compressible Navier-Stokes equations in general curvilinear coordinates using an accurate sixth-order compact scheme for derivatives and interpolations on a staggered grid (Nagarajan *et al.*, 2003).

An overset mesh procedure is employed in the simulation which uses two different types o grid: the first is an O-type grid block that surrounds the airfoil, and the second is a H-type (Cartesian) grid block applied to enclose the entire computational domain. The solution in each grid is integrated in time with different methods. The implicit second-order scheme of Beam and Warming (Beam and Warming, 1978) is used in the O-type grid to reduce the stiffness problem typical of boundary layers grids and, a third-order Runge-Kutta scheme is used to integrate in time the background H-type block. A fourth-order Hermite interpolation scheme is applied to exchange information in the overlapping zones of the overset procedure between the grid blocks (Bhaskaran and Lele, 2010).

A sixth-order compact filter (Lele, 1992) is applied in flow regions away from the solid boundaries in order to control numerical instabilities which may arise from mesh non-uniformities and interpolations between overlapping grids. The wall boundary conditions on the airfoil are defined as no-slip and adiabatic, and along the spanwise direction, periodic boundary conditions are used to enforce spanwise homogeneity. In the far-field, the boundary conditions are applied with Riemann invariants and a sponge layer is used in order to minimize acoustic waves reflections (Wolf, 2011). More information about the numerical procedure can be found in the works of Nagarajan *et al.* (2003), Bhaskaran and Lele (2010) and Wolf (2011). Furthermore the present numerical procedure has been validated for several 2-D and 3-D simulations of compressible airfoil flows at different conditions (see (Wolf *et al.*, 2012a,b, 2013; Ramos *et al.*, 2019; Ricciardi *et al.*, 2022; Miotto *et al.*, 2022; Lui *et al.*, 2022)).

2.2 Flow and grid details

The flow conditions of the simulations are defined as Reynolds number based on the inflow velocity and chord length $Re_c = 400,000$, and the freestrem Mach number is $M_\infty = 0.2$. The angle of attack of the airfoil is 9 deg. and the H-type block is generated such that there is no confinement effect of the computational domain in the flow. A random spanwise tripping is applied from $0.04 \leq x/c \leq 0.09$, which is the region where the natural transition initiates, in order to avoid the presence of two-dimensional Tolmien-Schilichting waves. Figure 1(a) presents a snapshot from the simulation where iso-surfaces of Q-criterion colored by x-momentum are shown.

The mesh is configured by an O-grid type block with $1200 \times 170 \times 144$ grid points and a H-type block with $960 \times 599 \times 72$ grid points resulting in a mesh with approximately 71 million grid points. The airfoil span is chosen to resolve 3 boundary layer thicknesses in order to minimize the effects of the periodic boundary conditions. Figure 2 present a full view of the mesh setup employed in the present simulation, only 10th grid point is displayed to have a better visualization of the mesh.

In order to assess the spatial resolution for the present LES, the grid resolution is measured in wall units which resulted in $\Delta x^+ < 40$, $\Delta y^+ < 1$, and $\Delta z^+ < 30$ along the entire suction side boundary layer, showing compliance with wall-resolved LES calculations as discussed by Georgiadis *et al.* (2010). Futhermore, we also try to avoid large stretching ratios along the streamwise and wall-normal directions to guarantee smooth metric terms, the maximum stretching factor is set as 4%. A hyperbolic grid generator is also employed to guarantee an orthogonal grid along the boundary layer region.

3. RESULTS AND DISCUSSION

The focus of this work is to understand the effects of APGs in TBL generated by an increased angle of attack. Therefore, some important parameters will be analized. Firstly, integral quantities of the boundary layer are investigated,

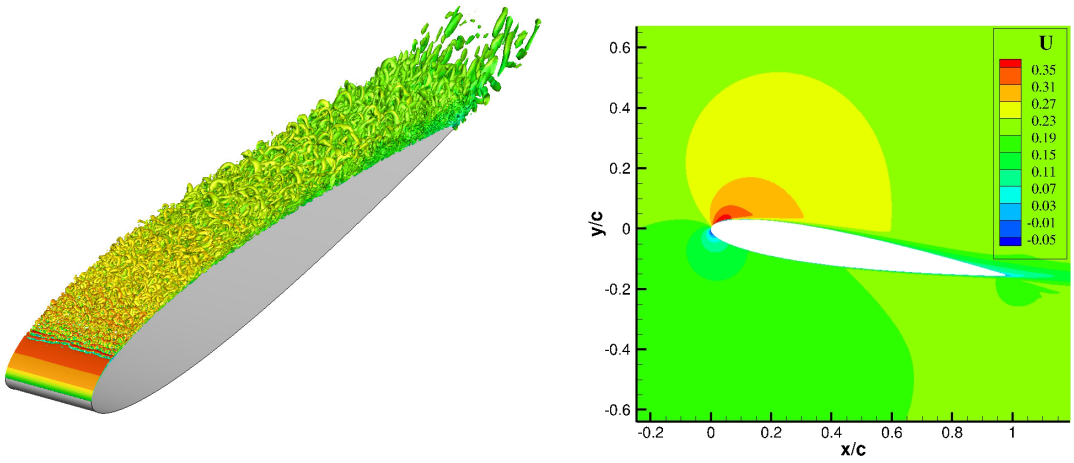

(a) Iso-sufaces of Q-criterion colored by x-momentum. (b) Spanwise and time-averaged u-velocity component.

Figure 1. Results from the simulation for a NACA0012 at AoA = 9 deg, $Re_c = 400,000$ and $M_\infty = 0.2$.

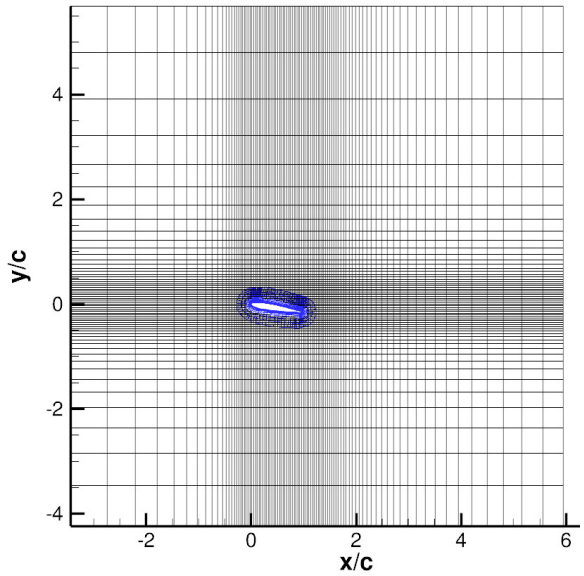

Figure 2. Full computational domain used in the simulation (every 10th grid point is shown).

including the displacement δ^* and the momentum thickness θ, and the Clauser pressure-gradient parameter β. Then, turbulence statistics such as the inner-scaled mean velocity profile, the Reylnolds stresses.

3.1 Integral quantities

Figure 3 presents the displacement thickness δ^* and the momentum thickness θ. For the purpose of obtain these parameters, the iterative method presented by Vinuesa *et al.* (2016) is used to determine the boundary layer thickness (δ). Figure 3 also shows a comparison between the LES results and the values calculated by Xfoil (Drela, 1989) where can be seen a great agreement between both results.

The displacement and momentum thicknesses allows the calculation of the Clauser pressure-gradient parameter β defined as $\beta(x) = \frac{\delta^*}{\tau_w}\frac{\mathrm{d}P_e}{\mathrm{d}x_t}$, which provides the magnitude of the pressure gradient. Here, τ_w is the wall shear stress and P_e is the pressure at the boundary-layer edge. Figure 4 presents the evolution along the airfoil chord of the Clauser parameter, where a sharp rise towards the trailing edge can be observed.

3.2 Turbulence statistics

The first analysis conducted in turbulence statistics is the analysis of the mean velocity profiles evaluated at different airfoil chord positions, where can be seen from Fig. 4 that each chord position has a different and increasing Clauser

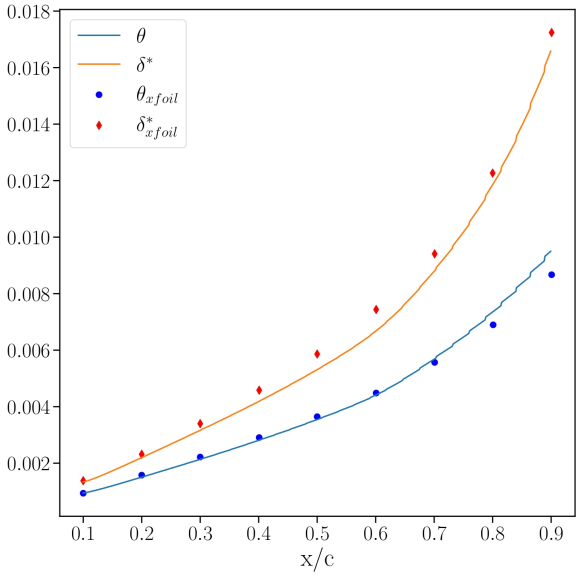

Figure 3. Chordwise evolution of displacement and momentum thicknesses.

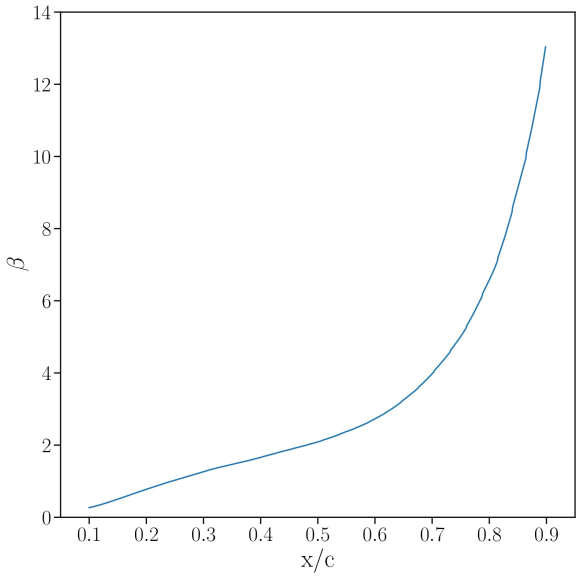

Figure 4. Evolution of the Clauser pressure-gradient parameter along the airfoil chord.

parameter. Figure 5 shows the the tangential mean-velocity profiles scaled by the friction velocity u_τ as a function of the wall-normal distance in wall units y^+. The red-dashed lines represent the values computed using the standard law of the wall for the viscous sublayer and the logarithmic region, where for the latter, $\kappa = 0.41$ and $B = 5.2$. The first observation that can be drawn from Fig. 5 is that the normalized tangential velocity (U_t^+) in the potential flow region is increasing along the chord, this observation is similar to that reported in the work of Spalart and Watmuff (1993) and Monty *et al.* (2011). Another region that is impacted by the APG is the log-layer regions, as can be observed from Fig. 5, it presents a vertical downward shift. This same trend was also observed by Spalart and Watmuff (1993). Moreover, the log law region is reduced in size as the APG increases as also observed by Monty *et al.* (2011). These observations are also similar to those presented by Lee and Sung (2008), demonstrating that the standard logarithmic law may not be valid for some APG flows.

Further remarks can be provided through the analysis of the Reynolds stresses tensor presented in Fig. 6, where the components are normalized by the friction velocity squared at different positions along the airfoil chord. The first finding to be noted relates to the tangential component $\langle u_t u_t \rangle^+$ in Fig. 6(a), which shows the emergence of a secondary peak in the outer region with an increasing APG. This behavior is also observed by Monty *et al.* (2011) and Vinuesa *et al.* (2017a) and can be explained by the interaction between the larger, most energetic scales of the boundary layer and the APG, which is felt throughout the boundary layer and results in a higher turbulence intensity (Vinuesa *et al.*, 2017a; Monty *et al.*, 2011). Moreover, when analysing the normal component $\langle u_n u_n \rangle^+$ presented in Fig. 6(b), it can be seen

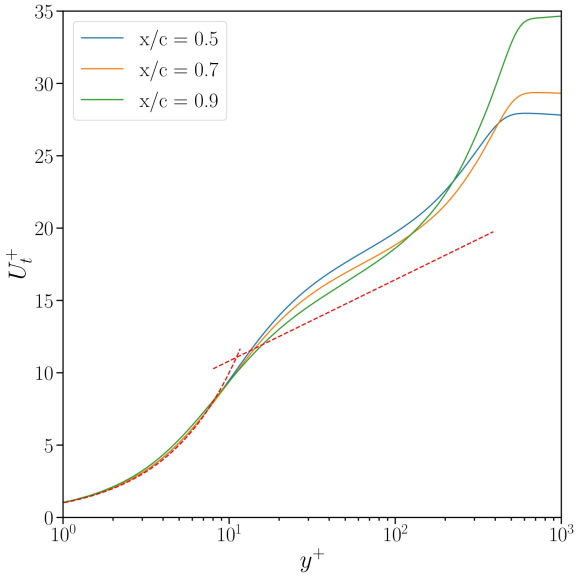

Figure 5. Inner-scaled tangential mean velocity profiles at different chord positions.

that the APG increases the wall normal velocity fluctuations in the outer layer, a behavior that contributes to the boundary layer thickening. In addition, this behavior also starts to affect regions towards the inner layer with an increasing APG. A significant increase is noticeable for all Reynolds stress components in the outer region when the APG increases, this being related to the energization of the boundary layer due to the APG (Harun *et al.*, 2013).

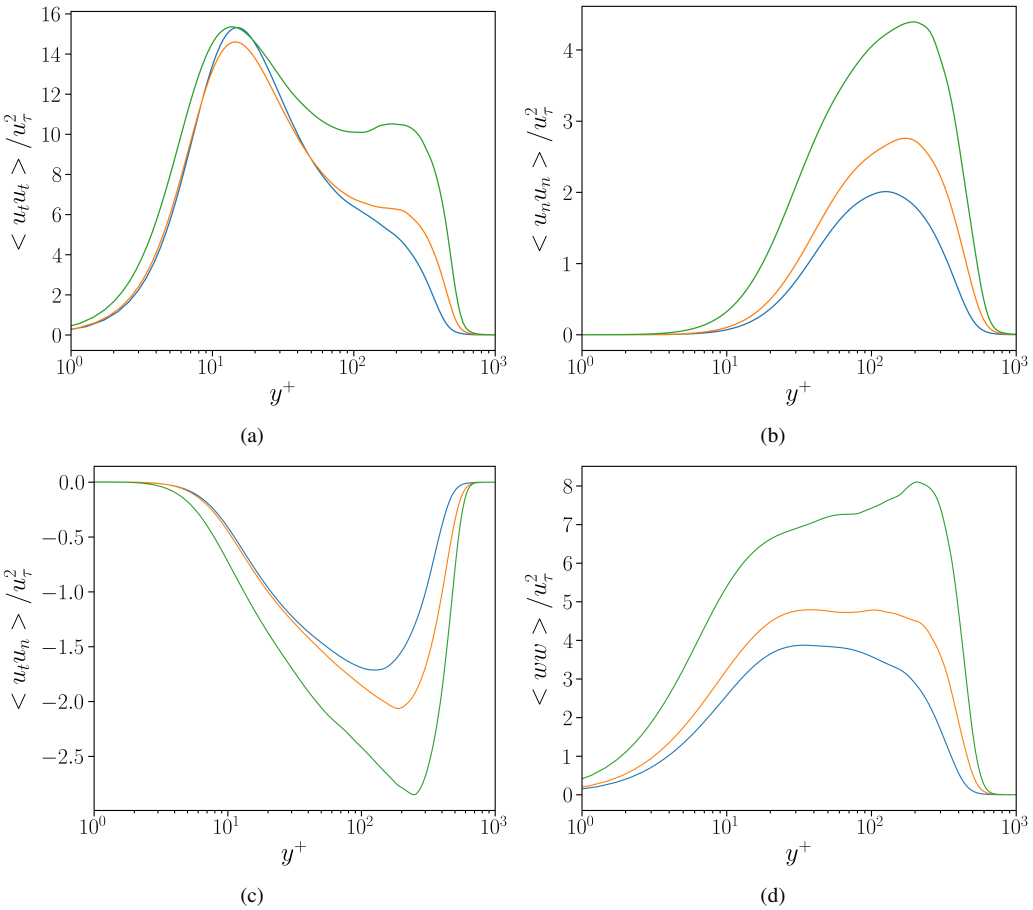

Figure 6. Inner-scaled Reynolds stress distributions at different airfoil chord positions. The colors represent positions on the airfoil chord: (—) $x/c = 0.5$, (—) $x/c = 0.7$ and (—) $x/c = 0.9$

4. CONCLUSIONS

In the present work, a wall-resolved LES of a NACA0012 airfoil at 9 deg. angle of attack is performed for $Re_c = 400,000$ and $M_\infty = 0.2$. Even though the angle of attack is high, there is no flow separation in the airfoil. The high angle of attack allows de development of a great adverse pressure gradients (APGs) in the turbulent boundary layer along the airfoil chord. The magnitude of the APGs is evaluated using the Clauser pressure-gradient parameter (β). Integral quantities are calculated in terms of displacement and momentum thicknesses. The turbulence quantities are shown in terms of the inner-scaled mean velocity and Reynolds stress profiles. The purpose of this study is to understand the effects of the APGs on turbulent boundary layers due to the angle of attack.

Firstly, we show the magnitude of the pressure-gradient through the Clauser parameter, where it can be seen a sharp increase in this parameter throughout the airfoil chord towards the trailing edge. This allows us to assess the inflence of different APG condition in each airfoil chord position. Then, we show that the inner-scaled mean velocity profile is greatly impacted by the APG. The inner-scaled velocity in the potential flow region increases with the APG, the log-layer shifts vertically downwards and also is reduced in size, as reported in the literature. Finally, we show that the Reynolds stress components are amplified with increasing APGs, with the tangential component ($\langle u_t u_t \rangle^+$) presenting an emergence of a secondary peak in the outer region and a major peak appears at the outer region for all the other components, an effect attributed in the literature due to an energization of the boundary layer by the APG.

5. ACKNOWLEDGEMENTS

The authors acknowledge the financial support received from Fundação de Amparo à Pesquisa do Estado de São Paulo, FAPESP, under Grants No. 2013/08293-7 and 2021/06448-0. FAPESP is also acknowledged for the scholarship provided to the first author under grant No. 2022/00256-4. The authors also thank the National Laboratory of Scientific Computing (LNCC/MCTI, Brazil) for providing the computational resources via SDumont cluster, where the numerical simulations were performed through project SimTurb.

6. REFERENCES

Beam, R.M. and Warming, R.F., 1978. "An implicit factored scheme for the compressible navier-stokes equations". *AIAA Journal*, Vol. 16, No. 4, pp. 393–402.

Bhaskaran, R. and Lele, S.K., 2010. "Large eddy simulation of free-stream turbulence effects on heat transfer to a high-pressure turbine cascade". *Journal of Turbulence*, Vol. 11, No. 6, pp. 1–15.

Bourassa, C. and Thomas, F.O., 2009. "An experimental investigation of a highly accelerated turbulent boundary layer". *Journal of Fluid Mechanics*, Vol. 634, pp. 359–404.

Bradshaw, P., 1967. "The turbulence structure of equilibrium boundary layers". *Journal of Fluid Mechanics*, Vol. 29, No. 4, pp. 625–645.

Clauser, F.H., 1954. "Turbulent boundary layers in adverse pressure gradients". *Journal of the Aeronautical Sciences*, Vol. 21, No. 2, pp. 91–108.

Clauser, F.H., 1956. "The turbulent boundary layer". *Advances in Applied Mechanics*, Vol. 4, pp. 1–51.

Drela, M., 1989. "Xfoil: An analysis and design system for low reynolds number airfoils". In *Low Reynolds number aerodynamics*, Springer, pp. 1–12.

Georgiadis, N.J., Rizzetta, P.D. and Fureby, C., 2010. "Large-eddy simulation: current capabilities, recommended practices, and future research". *AIAA Journal*, Vol. 48, No. 8, pp. 1772–1784.

Harun, Z., Monty, J.P., Mathis, R. and Marusic, I., 2013. "Pressure gradient effects on the large-scale structure of turbulent boundary layers". *Journal of Fluid Mechanics*, Vol. 715, pp. 477–498.

Lee, J. and Sung, H.J., 2008. "Effects of an adverse pressure gradient on a turbulent boundary layer". *International Journal of Heat and Fluid Flow*, Vol. 29, No. 3, pp. 568–578.

Lele, S.K., 1992. "Compact finite difference schemes with spectral-like resolution". *Journal of Computational Physics*, Vol. 103, No. 1, pp. 16–42.

Lui, H.F.S., Ricciardi, T.R., Wolf, W.R., Braun, J., Rahbari, I. and Paniagua, G., 2022. "Unsteadiness of shock-boundary layer interactions in a mach 2.0 supersonic turbine cascade". *Physical Review Fluids*, Vol. 7, No. 9, p. 094602.

Miotto, R.F., Wolf, W.R., Gaitonde, D. and Visbal, M., 2022. "Analysis of the onset and evolution of a dynamic stall vortex on a periodic plunging aerofoil". *J. Fluid Mech.*, Vol. 938, p. A24.

Monty, J.P., Harun, Z. and Marusic, I., 2011. "A parametric study of adverse pressure gradient turbulent boundary layers". *International Journal of Heat and Fluid Flow*, Vol. 32, No. 3, pp. 575–585.

Nagano, Y., Tagawa, M. and Tsuji, T., 1993. "Effects of adverse pressure gradients on mean flows and turbulence statistics in a boundary layer". In *Turbulent Shear Flows 8*, Springer, pp. 7–21.

Nagarajan, S., Lele, S.K. and Ferziger, J.H., 2003. "A robust high-order compact method for large eddy simulation". *Journal of Computational Physics*, Vol. 191, No. 2, pp. 392–419.

Ramos, B.L.O., Yeh, W.R.W.C. and Taira, K., 2019. "Active flow control for drag reduction of a plunging airfoil under deep dynamic stall". *Phys. Rev. Fluids*, Vol. 4, p. 074603.

Ricciardi, T.R., Wolf, W.R. and Taira, K., 2022. "Transition, intermittency and phase interference effects in airfoil secondary tones and acoustic feedback loop". *J. Fluid Mech.*, Vol. 937, p. A23.

Skåre, P.E. and Krogstad, P., 1994. "A turbulent equilibrium boundary layer near separation". *Journal of Fluid Mechanics*, Vol. 272, pp. 319–348.

Spalart, P.R. and Watmuff, J.H., 1993. "Experimental and numerical study of a turbulent boundary layer with pressure gradients". *Journal of Fluid Mechanics*, Vol. 249, pp. 337–371.

Tanarro, Á., Vinuesa, R. and Schlatter, P., 2020. "Effect of adverse pressure gradients on turbulent wing boundary layers". *Journal of Fluid Mechanics*, Vol. 883, p. A8.

Vinuesa, R., Bobke, A., Örlü, R. and Schlatter, P., 2016. "On determining characteristic length scales in pressure-gradient turbulent boundary layers". *Physics of Fluids*, Vol. 27, No. 5, p. 055101.

Vinuesa, R., Hosseini, S.M., Hanifi, A., Henningson, D.S. and Schlatter, P., 2017a. "Pressure-gradient turbulent boundary layers developing around a wing section". *Flow, Turbulence and Combustion*, Vol. 99, No. 3, pp. 613–641.

Vinuesa, R., Örlü, R., Vila, C.S., Ianiro, A., Discetti, S. and Schlatter, P., 2017b. "Revisiting history effects in adverse-pressure-gradient turbulent boundary layers". *Flow, Turbulence and Combustion*, Vol. 99, No. 3, pp. 565–587.

Wolf, W.R., Azevedo, J.L.F. and Lele, S.K., 2012a. "Convective effects and the role of quadrupole sources for aerofoil aeroacoustics". *J. Fluid Mech.*, Vol. 708, pp. 502—-538.

Wolf, W.R., Azevedo, J.L.F. and Lele, S.K., 2013. "Effects of mean flow convection, quadrupole sources and vortex shedding on airfoil overall sound pressure level". *J. of Sound and Vibration*, Vol. 332, pp. 6905–6912.

Wolf, W.R., Lele, S.K., Jothiprasad, G. and Cheung, L., 2012b. "Investigation of noise generated by a DU96 airfoil". In *18th AIAA/CEAS Aeroacoustics Conference (33th AIAA Aeroacoustics Conference), AIAA Paper 2012-2055*. pp. 1–15.

Wolf, W.R., 2011. *Airfoil aeroacoustics: LES and acoustic analogy*. Ph.D. thesis, Stanford University, Stanford, California.

7. RESPONSIBILITY NOTICE

The authors are solely responsible for the printed material included in this paper.